Available online at www.sciencedirect.com
ScienceDirect
Ceramics International 37 (2011) 1653–1660
CERAMICS INTERNATIONAL
www.elsevier.com/locate/ceramint

Experimental and theoretical dielectric studies of PVDF/PZT nanocomposite thin films

A.K. Zak [a,b,*], W.C. Gan [a], W.H. Abd. Majid [a], Majid Darroudi [b], T.S. Velayutham [a]

[a] Low Dimensional Material Research Center, Department of Physics, Faculty of science, University of Malaya, Kuala Lumpur 50603, Malaysia
[b] Department of Chemistry, Faculty of Science, Ferdowsi university of Mashhad, 91775-1436 Mashhad, Iran

Received 19 November 2010; received in revised form 13 December 2010; accepted 22 January 2011
Available online 18 February 2011

Abstract

Poly(vinylidene fluoride)/lead zirconate titanate nanocomposite thin films (PVDF/PZT-NPs) were successfully prepared by mixing fine $Pb(Zr_{0.52},Ti_{0.48})O_3$ nanoparticles (PZT-NPs) into a PVDF solution under ultrasonication. The mixture was spin coated onto glass substrate and then cured at 110 °C. X-ray diffraction (XRD), transmission electron microscopy (TEM), and scanning electron microscopy (SEM) were used to characterize the structure and properties of the obtained thin-film nanocomposites. The dielectric properties of the PVDF/PZT-NPs were analyzed in detail with respect to frequency. In comparison with pure poly (vinylidene fluoride), the dielectric constant of the nanocomposite (15 vol.% PZT-NPs) was significantly increased, whereas the loss tangent was unchanged in the frequency range of 100 Hz to 30 MHz. The nanocomposites exhibited good dielectric stability over a wide frequency range. Different theoretical approaches were employed to predict the effective dielectric constants of the thin film nanocomposite systems, and the estimated results were compared with the experimental data.

Keywords: B. Nanocomposites; C. Dielectric properties; D. PZT; PVDF

1. Introduction

''Smart materials'' are materials that show reproducible and stable responses through significant variations of at least one property when subjected to external stimuli [1,2]. Ceramic–polymer composites constitute a new class of construction and functional materials of great application potential in having the combined hardness and stiffness of ceramics and the elasticity, flexibility, low density, and high breakdown strength of polymers. Consequently, ceramic–polymer composites are being increasingly utilized for their specific dielectric, ferroelectric, piezoelectric, pyroelectric, electro-optic, and superconducting properties in microdevices [3]. When polymeric materials serve for practical uses, they are commonly mixed with other materials to achieve the desired performance. One of the best piezo- and pyroelectric polymers is the semicrystalline polymer poly(vinylidene fluoride) (PVDF) [4]. To achieve various performance objectives, high-dielectric-constant ferroelectric ceramics such as $Pb(Mg_{1/3}Nb_{2/3})O_3$-$PbTiO_3$ (PMN-PT) [5], $Pb(Zr,Ti)O_3$ (PZT) [6], LTNO [7], $CaCu_3Ti_4O_{12}$ (CCT) [8] and $BaTiO_3$ (BT) [9] have been used as fillers in polymers by previous researchers. Similarly, metallic fillers have also been used to achieve ultrahigh dielectric constants in metal–polymer composites or three-phase composite systems [10–12]. The high dielectric constant of the ceramic allowed for a high dielectric constant and a strong piezoelectric effect in the composite for moderate volume fractions of the ceramic filler. The dielectric properties of these composites can be controlled over a broad range by inorganic inclusions [13]. In 1979, Furukawa et al. [14] published a study on the effect of the addition of ceramic particles in various polymer/PZT 3-dimensional systems. For the PVDF/PZT composites, the authors concluded that the piezoelectric effect originated in the ceramic particles unless the volume fraction of the PZT was very small. Later, Yamada et al. [15] developed expressions to predict the dielectric and piezoelectric constants and the elastic modulus of binary systems such as PVDF/PZT composites.

In the present study, the polymeric material used to prepare the nanocomposite thin films was poly(vinylidene fluoride)

* Corresponding author at: Low Dimensional Material Research Center, Department of Physics, Faculty of science, University of Malaya, Kuala Lumpur 50603, Malaysia. Tel.: +60 12 2850849.
E-mail address: alikhorsandzak@gmail.com (A.K. Zak).

0272-8842/$36.00
doi:10.1016/j.ceramint.2011.01.037

Table 1
PVDF, PVDF\PZT, and PZT-NPs specimen dimensions and dielectric properties at 100 Hz.

Sample	Thickness, d (m)	Area, A (m^2)	Capacity, C (F) 100 Hz	Dielectric constant ε_r 100 Hz
PVDF	277×10^{-9}	4×10^{-6}	9.99×10^{-10}	7.82
PVDF\PZT	352×10^{-9}	4×10^{-6}	1.11×10^{-9}	11.10
PZT-NPs	3.278×10^{-3}	1.308×10^{-4}	1.03×10^{-9}	2916.84

(PVDF), and the ceramic material was lead zirconate titanate nanoparticles (PZT-NPs, with a diameter of ~20 nm). Both materials are dielectric but with quite different characteristics. PVDF has a low density (ρ = 1780 kg/m^3) compared to the PZT (ρ = 7500 kg/m^3); the PZT-NPs have a high dielectric constant ($\varepsilon_r > 2800$ at 100 kHz) compared to the PVDF ($\varepsilon_r = 12$) [4]. The frequency dependence of the electrical properties of the PVDF/PZT nanocomposite thin films was studied in the frequency range of 100 Hz to 40 MHz. In previous studies, for example Furukawa et al. [14] and Firmino et al. [6], constant values of ceramic particles permittivity were examined over the entire frequency range to investigate the permittivity of the composites. In this work, the permittivity of the PZT-NPs was measured as a function of frequency, and the dielectric properties of the PVDF/PZT nanocomposites were investigated by experimental and theoretical approaches.

2. Experimental

2.1. Preparation of PVDF/PZT nanocomposite thin films

The PZT-NP [$Pb(Zr_{0.52},Ti_{0.48})O_3$] powder was prepared by a sol–gel method. Titanium isopropoxide, zirconium n-propoxide and lead acetate were used as starting materials, and 2-methoxyethanol was used as a solvent. The gel was dried, then calcined at temperatures of 600 °C, 650 °C or 700 °C for 1 h to obtain fine yellow PZT-NPs powders [16]. The PZT-NPs powders was sonicated and dispersed in ethyl methyl ketone (EMK). Simultaneously, PVDF powder (Sigma–Aldrich) was dissolved in the EMK at 60 °C and stirred for 2 h. Next, the dispersed PZT-NPs were added to the PVDF solution and stirred for 2 h at 60 °C. The initial concentration of the solution was 0.2 g PVDF per 15 ml of EMK and the PVDF/PZT-NPs ratio was 85/15. The PVDF/PZT-NPs solution was coated onto a glass electrode substrate by a spin-coating method at 1500 rpm for 30 s. The samples were then heated in an oven at 60 °C for 1 h to remove the solution and subsequently annealed on a hot plate at 110 °C for 1 h. Finally, the top electrode was coated onto the samples using a thermal evaporator (Edward 306).

2.2. Characterization techniques

X-ray diffraction (XRD) studies were carried out using a Siemens D5000 diffractometer with Cu $K\alpha_1$ radiation (λ = 0.154056 nm) over a wide range of 2θ ($5^\circ \leq 2\theta \leq 80^\circ$). The microstructure and the morphology of the samples were characterized using scanning electron microscopy (SEM, FEI Quanta 200 FESEM) and transmission electron microscopy (TEM, Hitachi H-7100). FTIR (ST-IR\ST-SIR spectrometer) was used to study of the normal vibration modes of PVDF. To measure the permittivity of the PZT-NPs, they were pressed under 200 MPa pressure then the PZT-NPs pellet was electroded with silver paint and cured at 60 °C for 1 h. The capacitance of the electrode specimen was measured as a function of frequency (100 Hz to 40 MHz) using an impedance analyzer (HP 4194A) at room temperature, and the dielectric constant was evaluated from $C = \varepsilon_o \varepsilon_r A/d$, were C is the capacitance, ε_r is the dielectric constant, A is the surface area, d is the sample thickness and ε_o is the permittivity of vacuum. The thickness of the thin films was measured by a mechanical profiler (P-6 KLA-Tencor); the results are presented in Table 1. Theoretical models, i.e., Maxwell's, Clausius-Mossotti, Effective Medium Theory, Furukawa, Rayleigh and Yamada, were employed to rationalize the dielectric behavior of the composites under investigation.

3. Results and discussion

3.1. X-ray diffraction analysis

The X-ray powder diffraction patterns obtained for the PZT-NPs calcined at temperatures of 700 °C is shown in Fig. 1. PZT-NPs having a pure perovskite structure were obtained at this calcination temperature. The Scherrer method was used to calculate the crystalline size of the PZT-NPs, and it was found to be ~17 nm. The X-ray diffraction pattern of the PVDF and PVDF/PZT nanocomposite thin films is shown in Fig. 2. It was estimated from these patterns that the PVDF (Fig. 2a) existed in

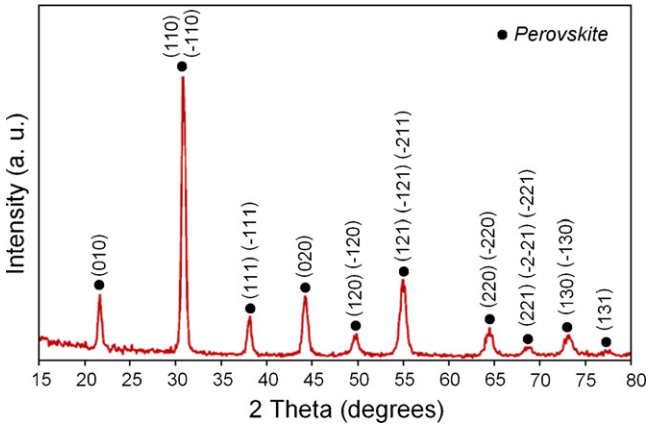

Fig. 1. X-ray diffraction patterns for PZT-NPs calcined at different temperatures. The pure perovskite phase was achieved at 700 °C.

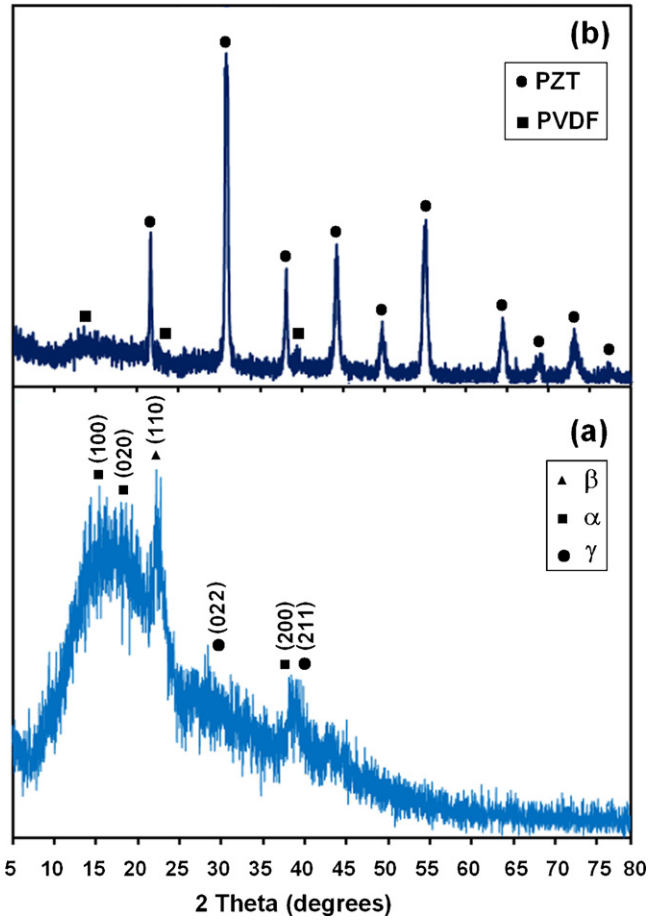

Fig. 2. X-ray diffraction patterns for (a) PZT-NPs, (b) pure PVDF, and (c) PVDF/PZT-NPs. The pattern of pure PVDF shows exists of α, β and γ phase in the compound.

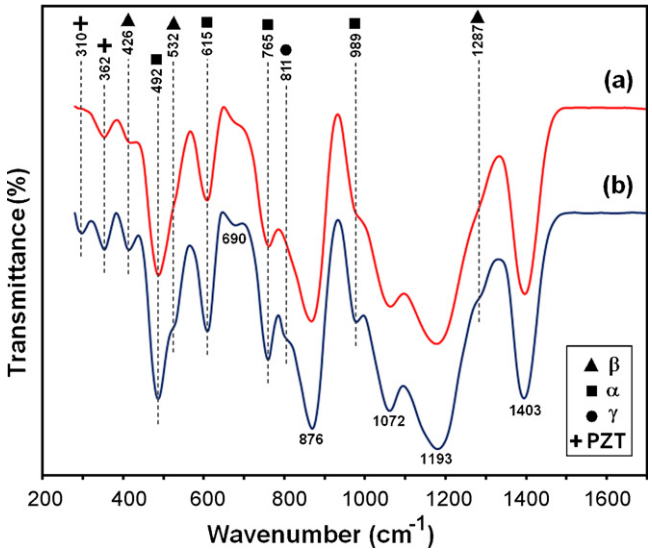

Fig. 3. FTIR traces for (a) pure PVDF and (b) PVDF/PZT-NPs. The results show exists of α, β and γ phase in the compound.

mixed α, β and γ phases. The peaks at 2θ corresponding to 17.5° (1 0 0), 18.0° (0 2 0), and 38.1° (2 0 0) were assigned to the α-PVDF, 22.2° (1 1 0) was assigned to the β-PVDF, whereas the peaks at $2\theta = 26.4°$ (0 2 2) could be indexed to the γ-PVDF [8,17]. The X-ray diffraction pattern obtained for the PVDF/PZT-NPs (Fig. 2b) clearly shows the PZT diffraction peaks.

3.2. FTIR study of the PVDF and PVDF/PZT-NPs

In Fig. 3, FTIR transmittance spectra of PVDF (a) and PVDF/PZT (b) are shown in the range of 285–1700 cm^{-1}. The identified reigns are rich in information on the conformational isomerism of the chain, providing information on α and β phase content. The absorption bands at 426, 532, and 1287 cm^{-1} are related to β-phase characteristic bands [18]. The band at 1287 and 532 cm^{-1} are assigned to CH_2 and CF_2 bending vibration bands, respectively. The mode at 426 cm^{-1} is parallel to *a*-axis of PVDF chain.

The α-phases are observed at 492, 615, 765, and 989 cm^{-1} [18]. The absorption band at 765 cm^{-1} can be related to a rocking vibration in the PVDF chain. The bending vibration of CF_2 is observed at 615 cm^{-1} also, bending and wagging vibration of CF_2 groups ascribed to the α-PVDF polymorph are detected at 492 cm^{-1} [19].

The absorption bonds at 310 and 362 cm^{-1} are attributed to Ti, Zr–O normal vibration modes, also, there is C–H stretching vibration mode at 362 cm^{-1} [16]. The γ-phase is estimated from the band occurred at 811 cm^{-1} [18]. The results which obtained from FTIR are summarized in Table 2.

3.3. Morphology study of the PVDF and PVDF/PZT-NPs

Fig. 4a shows a transmission electron micrograph of the PZT-NPs. The average initial size of the PZT-NPs was ~24 nm, as evidenced by the TEM micrographs. The surface morphology of the PVDF/PZT-NPs, dried PVDF, and annealed PVDF revealed by scanning electron microscopy (SEM) are shown in Fig. 4b, c, and d respectively. The SEM image of the composites (Fig. 4b) shows the excellent distribution of the PZT-NPs fillers within the PVDF matrix. The morphology of the dried PVDF (Fig. 4c) and the annealed PVDF (Fig. 4d) indicate that the lamellas were formed during the annealing process. As it shown in Fig. 5, the lamellas start growing from a nucleus of a crystal. A slow diffusion leads to tree-like architecture of branches and twigs with built-in depletion zones [20].

3.4. Experimental study of the frequency dependence of the dielectric constant

Fig. 6 presents the variation of dielectric constant and loss with frequency for the PZT-NPs calcined at 700 °C for 1 h. The dielectric constant and the loss value start from 2917 and 3.67, respectively, at 100 Hz, and then decrease to 330 and 0.08 as the frequency increases to 31 MHz. A resonance accurse at 38 MHz above this frequency, the value of the dielectric constant and the loss decreases again as frequency increases. The frequency dependence of the dielectric constant and loss of the nanocomposite thin films with 15% PZT-NPs and pure

Table 2
Characteristic bands with specific vibrational modes and crystalline phases.

Wave number cm^{-1}	Group	Vibration	Comments	Ref.
310	(Zr, Ti)–O	Stretching		[16]
	C–H	Stretching		
362	(Zr, Ti)–O	Bending		[16]
426			β-Phase	[18]
492	CF_2	Bending and wagging	α-Phase (in-phase combination)	[24]
532	CF_2	Bending	β-Phase	[18]
615	CF_2 and C–C–C	CF_2 bending and C–C–C skeletal vibration	α-Phase	[24]
690			Presence of head to head and tail to tail configurations	[24]
765		In-plane bending Or rocking	α-Phase	[24]
811			γ-Phase	[18]
876	CH_2 and CF_2	CH_2 rocking and CF_2 stretching	β-Phase	[18]
989			α-Phase	[18]
1072	C–C–C	Bending		[24]
1193	CH_2	Wagging	β-Phase	[18]
1287	CH_2	Rocking	β-Phase or γ-Phase	[18,24]
1403	CH_2	In-plane bending Or scissoring		[24]

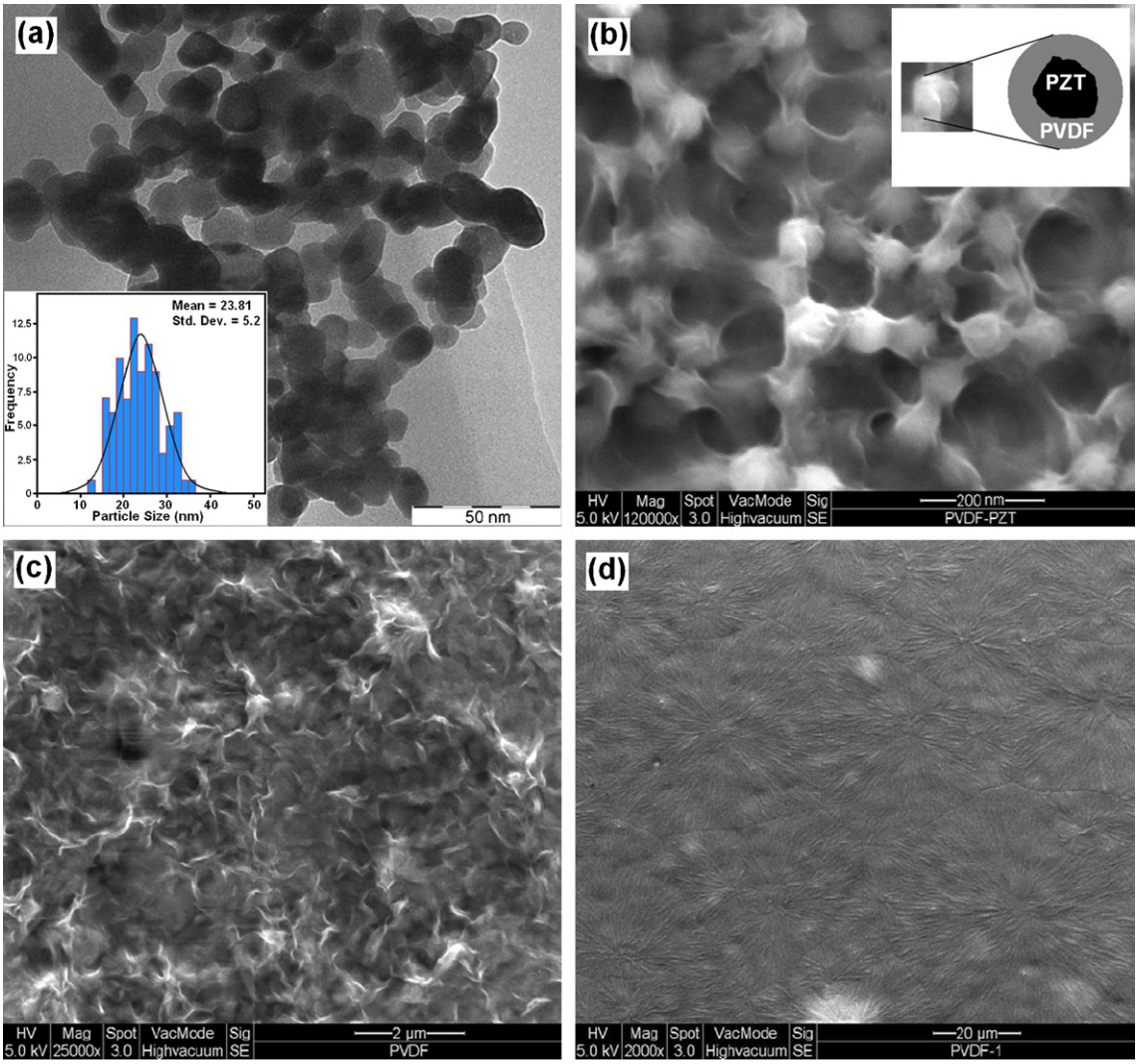

Fig. 4. TEM morphology of the PZT-NPs (a), SEM micrographs of PVDF/PZT-NPs film (b), dried PVDF film (c), and PVDF film annealed at 110 °C. The inset image of (b) shows the coverage of the polymer surrounding the nanoparticles.

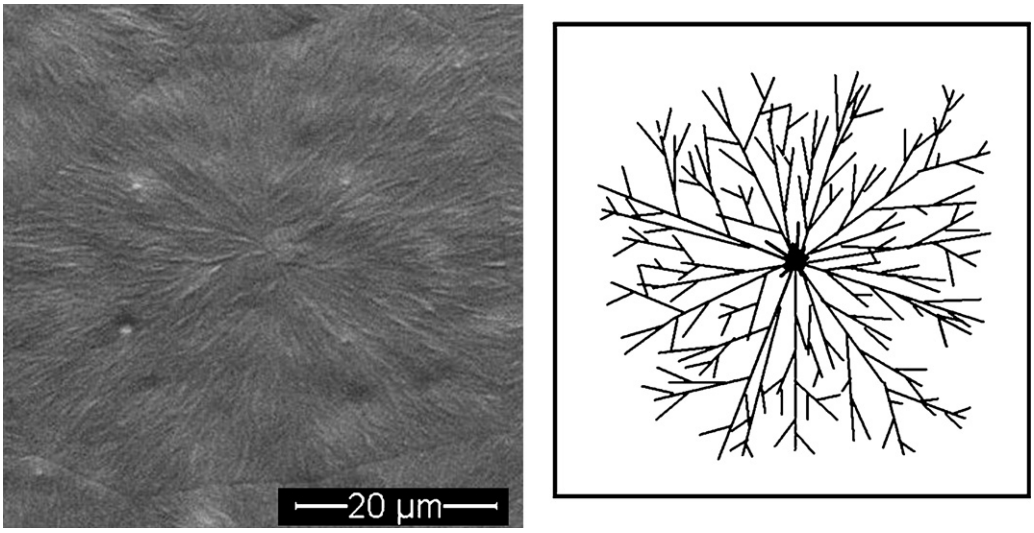

Fig. 5. Crystallization starts from a nuclus of a crystal and grows in a blend melt with a tree-like architecture.

PVDF are shown in Figs. 7 and 8, respectively. As expected, the effective dielectric constant (ε) was increased at all frequency as the PZT-NPs were added to the matrix under study. The effective dielectric constant obtained was higher than that of pure PVDF but much lower than that of the pure PZT-NPs. The low dielectric constant of the PVDF/PZT-NPs thin films compared to the PZT-NPs may be due to the causes apart from the connectivity and particle-size effects. Based on the X-ray studies, it was confirmed that PVDF is present as mixed α and γ phases, which are both nonpolar. Due to the nonpolar nature of PVDF, and the constrained polymer chain hindering the formation of electrical polarization, the value of ε is lower than that of PZT-NPs [8].

It was observed that the dielectric loss decreased as frequency increased for both pure PVDF and PVDF/PZT nanocomposite thin films from 100 Hz to 15 MHz, but increased as frequency increased further up to 39 MHz (Fig. 8). The inset of Fig. 8 shows that the frequency dependence of the dielectric loss of the pure PVDF and the PVDF/PZT nanocomposite were almost same in the frequency range of 100 Hz to 30 MHz. This suggests that the PVDF molecular chains play a more important role in this frequency range but that above 30 MHz the PZT-NPs play the main role in the dielectric loss behavior of the PVDF/PZT nanocomposite thin films.

3.5. Theoretical study of the dielectric behavior of PVDF/PZT nanocomposite thin films

To better understand the nature of the dielectric response of the composite material with increasing ceramic concentration, several theoretical models were employed. The first model developed to predict the dielectric behavior of the composites was proposed by Maxwell in 1904 [21]; this model is still widely used. In this model, the dielectric response of the composite is given by:

$$\varepsilon = \frac{((2/3) + (\varepsilon_2/3\varepsilon_1)) + \alpha_2\varepsilon_2}{\alpha_1((2/3) + (\varepsilon_2/3\varepsilon_1)) + \alpha_2} \quad (1)$$

where ε_1 is the dielectric constant of the polymer, ε_2 is the dielectric constant of the filler, and α_1, α_2 are the volume fractions of the polymer and filler, respectively.

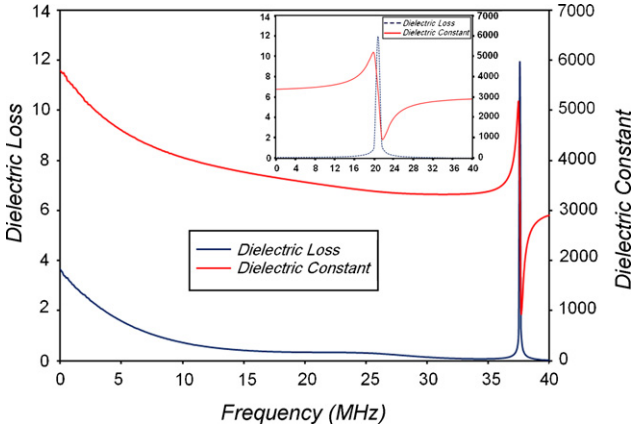

Fig. 6. The experimental dielectric constant and loss of the PZT-NPs as a function of frequency at room temperature, from 100 Hz to 40 MHz. The inset shows the resonance area.

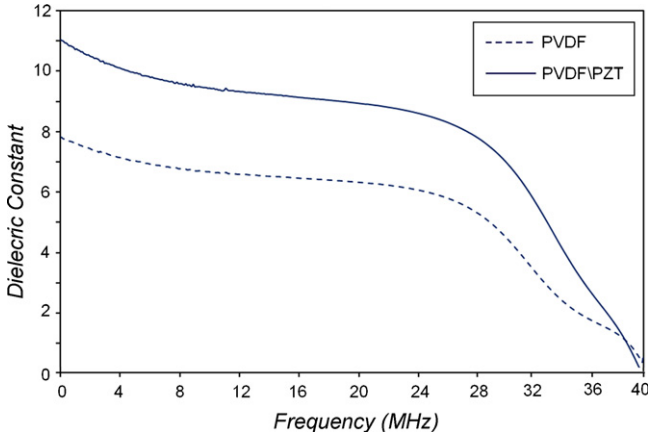

Fig. 7. The experimental dielectric constant of the pure PVDF and PVDF\PZT-NPs as a function of frequency at room temperature, from 100 Hz to 40 MHz.

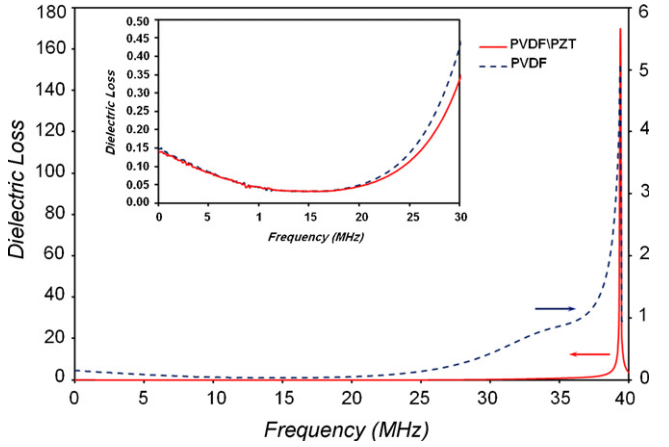

Fig. 8. The experimental dielectric loss of the pure PVDF and PVDF\PZT-NPs as a function of frequency at room temperature, from 100 Hz to 40 MHz. The inset shows that the loss value of PVDF\PZT and PVDF are almost same in frequency range of 100 Hz to 30 kHz.

In 1979, Furukawa et al. [14] derived an expression for biphasic composites with 0–3 connectivity. This model also assumes that the particles are spherical and uniformly dispersed throughout the polymer matrix. The entire system is dielectrically homogeneous and the response depends on the dielectric constant of the matrix. The dielectric behavior of the composite can be obtained from the following relation:

$$\varepsilon = \frac{1+2\alpha}{1-\alpha}\varepsilon_1 \tag{2}$$

where ε_1 is the dielectric constant of the matrix, ε is the effective dielectric constant and α is the volume fraction of the ceramic particles.

The Maxwell and Furukawa theories were used as the basis for a new theory that was presented by Rayleigh [22]. The Rayleigh equation correctly predicts the increase in permittivity

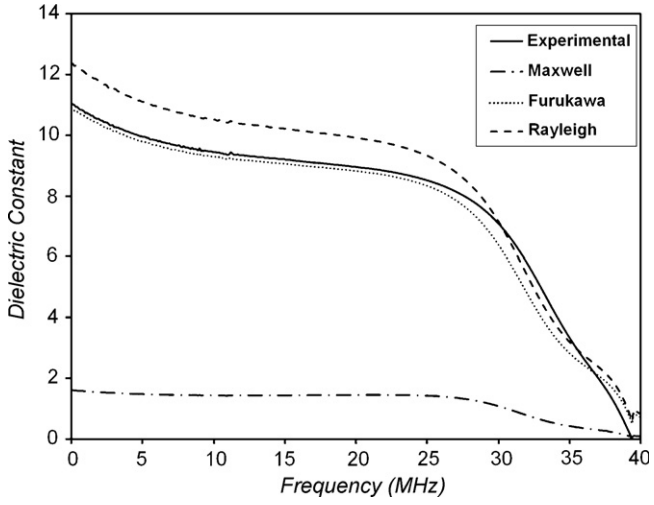

Fig. 9. Dielectric constant of PVDF\PZT-NPs obtained from experimental test and theoretical calculation (Furukawa, Maxwell and Rayleigh theories) at room temperature, from 100 Hz to 40 MHz.

when a small amount of inclusions are added to the matrix. In this model, the dielectric behavior of the composites is given by:

$$\varepsilon = \varepsilon_1\left(\frac{2\varepsilon_1+\varepsilon_2+2\alpha(\varepsilon_2-\varepsilon_1)}{2\varepsilon_1+\varepsilon_2-\alpha(\varepsilon_2-\varepsilon_1)}\right) \tag{3}$$

where ε_1 and ε_2 are the dielectric constants of the matrix and ceramic particles, respectively, ε is the effective dielectric constant and α is the volume fraction of the ceramic particles.

Fig. 9 shows the typical experimental and theoretical permittivities of the PVDF/PZT nanocomposite thin films. It can be seen here that dielectric permittivity measured at lower frequencies (below 100 Hz) was always greater than that measured at higher frequency. The dielectric constant decreased slowly with increasing frequency up to 25 MHz, and with further frequency increase the dielectric constant decreased very rapidly up to 40 MHz, the upper limit of the frequency range in this study. It was also observed that the results of the Furukawa theory were almost the same as the experimental results observed in the frequency range of 100 Hz to 25 MHz. There was an ~8% deviation between the results of the Rayleigh theory calculations and the experimental results, but the results of the Maxwell calculations were very different from the experimental results in this frequency range. These theories are based on a spherical morphology of the ceramic particles. Due to the nonspherical morphology of the PZT-NPs (see Fig. 4a), the theoretical calculations of the dielectric constant were not completely in accord with the experimental results. Above 25 MHz, the Rayleigh theory seems to be more reliable for calculating the dielectric constant compared to the others. In this case, the results showed that the Maxwell and Garnett theory was not a suitable theory for calculating the dielectric constant of the PVDF/PZT nanocomposite thin films.

In the effective medium theory (EMT) [23] and Yamada et al. [15] theory, the morphology of the particles is considered in the calculation of the dielectric constant. By the EMT method, the dielectric constant of the composite can be estimated from the following equation:

$$\varepsilon = \varepsilon_1\left(1+\frac{\alpha(\varepsilon_2-\varepsilon_1)}{\varepsilon_1+\eta(1-\alpha)(\varepsilon_2-\varepsilon_1)}\right) \tag{4}$$

where ε_1 and ε_2 are the dielectric constants of the matrix and ceramic particles, ε is the effective dielectric constant, α is the volume fraction of the ceramic particles and n is the fitting factor.

The value of n depends on the morphology of the particles. When the morphology of the particles is almost spherical, then the value of n is very small. A high value of n indicates largely nonspherically shaped particles. The experimental values in the frequency range of 100 Hz to 27 MHz were well fit by the EMT model with the shape parameter $n = 0.47$.

According to Yamada's model the dielectric constant is obtained from:

$$\varepsilon = \varepsilon_1\left(1+\frac{k\alpha(\varepsilon_2-\varepsilon_1)}{k\varepsilon_1+(1-\alpha)(\varepsilon_2-\varepsilon_1)}\right) \tag{5}$$

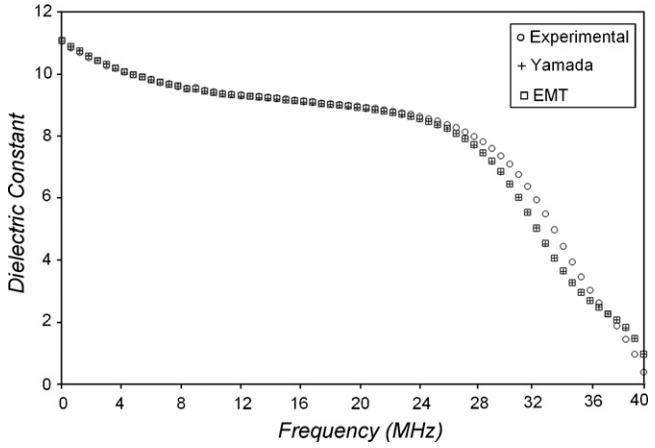

Fig. 10. Dielectric constant of PVDF\PZT-NPs obtained from experimental test and theoretical calculation (Yamada and EMT theories) at room temperature, from 100 Hz to 40 MHz.

where k is the parameter related to the morphology of the particles.

It is clear that for $k = 1/n$ Eqs. (4) and (5) are equal. Thus, the results of this theory would be the same as obtained from the EMT when $k = 2.13$. The difference between the experimental data and the predicted values was close to zero in the frequency range of 100 Hz to 27 MHz, but the difference increased to 5% in the high-frequency range from 27 MHz to 40 MHz. The difference can be related to the resonance frequency of the nanoparticles (see Fig. 6) because the resonance behavior of the PZT-NPs is affected by the polymer matrix. The results are shown in Fig. 10.

4. Conclusions

Nanocomposite thin films of PVDF/PZT with a PZT-NP content of 15% were fabricated and characterized. The XRD and TEM results showed that the particle size of the PZT-NPs was about 24 nm, and the SEM of the composites revealed an excellent distribution of PZT-NPs fillers within the PVDF matrix. As expected, the effective dielectric constant (ε) of PVDF was increased when it was mixed with PZT-NPs over the entire frequency range. The dielectric loss remained constant in the frequency range from 100 Hz to 30 kHz. However, as the frequency was increased above 30 kHz, the dielectric constant for the PVDF/PZT was higher than the pure PVDF. The results showed that the dielectric constant of the PVDF/PZT-NPs nanocomposite was increased by about 40% above that of pure PVDF. Among the various models used for rationalizing the dielectric behavior, it was found that in the frequency range from 100 Hz to 27 MHz the experimental data were comparable with those obtained from the EMT model (with $n = 0.47$) and the equivalent Yamada model (with $k = 2.13$). The discrepancy between the experimental data and the predicted value was less than 5% in the frequency range from 27 MHz to 40 MHz.

However, all these models have their limitations, as the interfacial structure and chemistry have not been taken into account. For example, the difference between the response predicted by the Yamada and EMT theories and the experimental data at high frequency can be attributed to the resonance frequency of the PZT-NP occurring in this range.

Acknowledgments

This work was supported by University Malaya (grant no: PS331/2009C, IPPP), Also, authors are thankful from University Malaya Chancellery for supporting this project by the High Impact Research grant: UM.C/625/1/HIR/041.

References

[1] C.A. Rogers, Intelligent material systems, the dawn of a new materials age, J. Intell. Mater. Syst. Struct. 4 (1993) 4–12.
[2] R.E. Newnham, G.R. Ruschau, Electromechanical properties of smart materials, J. Intell. Mater. Syst. Struct. 4 (1993) 289–294.
[3] M. Goel, Recent developments in electroceramics: MEMS applications for energy and environment, Ceram. Int. 30 (2004) 1147–1154.
[4] A.J. Lovinger, Developments in Crystalline Polymers, Elsevier, London, 1982.
[5] Z. Xu, F. Chen, Z. Xi, Z. Li, L. Cao, Y. Feng, X. Yao, The studies of single crystal PMN-PT68/32/polymer 1-3 composites, Ceram. Int. 30 (2004) 1777–1780.
[6] S. Firmino Mendes, C.M. Costa, V. Sencadas, J. Serrado Nunes, P. Costa, J.R. Gregorio, S. Laneros-Mendes, Effect of the ceramic grain size and concentration on the dynamical mechanical and dielectric behavior of poly(vinilidene fluoride)/$Pb(Zr_{0.53}Ti_{0.47})O_3$ composites, Appl. Phys. A 96 (2009) 899–908.
[7] Z.M. Dang, C.W. Nan, Dielectric properties of LTNO ceramics and LTNO/PVDF composites, Ceram. Int. 31 (2005) 349–351.
[8] P. Thomas, K.T. Varughese, K. Dwarakanath, K.B.R. Varma, Dielectric properties of pol(vinylidene fluoride)/$CaCu_3Ti_4O_{12}$ composites, Compos. Sci. Technol. 70 (2010) 539–545.
[9] F. Fang, W. Yang, M.Z. Zhang, Z. Wang, Mechanical response of barium–titanate/polymer 0-3 ferroelectric nano-composite film under uniaxial tension, Compos. Sci. Technol. 69 (2009) 602–605.
[10] L. Qi, B.I. Lee, S. Chen, W.D. Samuels, G.J. Exarhos, High-dielectric-constant silver–epoxy composites as embedded dielectrics, Adv. Mater. 17 (2005) 1777–1781.
[11] H.W. Choi, Y.W. Heo, J.H. Lee, J.J. Kim, H.Y. Lee, E.T. Park, Effects of $BaTiO_3$ on dielectric behavior of $BaTiO_3$–Ni–polymethyl methacrylate composites, Appl. Phys. Lett. 89 (2006) 132910.
[12] Z.M. Dang, Y.H. Lin, C.W. Nan, Novel ferroelectric polymer composites with high dielectric constants, Adv. Mater. 15 (2003) 1625–1629.
[13] H. Chen, X. Dong, T. Zeng, Z. Zhou, H. Yang, The mechanical and electric properties of infiltrated PZT/polymer composites, Ceram. Inter. 33 (2007) 1369–1374.
[14] T. Furukawa, I. Ishida, E. Fukada, Piezoelectric properties in the composite systems of polymers and PZT ceramics, J. Appl. Phys. 50 (1979) 4904–4912.
[15] T. Yamada, T. Ueda, T. Kitayama, Piezoelectricity of a high-content lead zirconate titanate/polymer composite, J. Appl. Phys. 53 (1982) 4328–4332.
[16] A. Khorsand Zak, W.H. Abd., Majid, Characterization and X-ray peak broadening analysis in PZT nanoparticles prepared by modified sol–gel method, Ceram. Inter. 36 (2010) 1905–1910.
[17] W. Ma, J. Zhang, S. Chen, X. Wang, b-Phase of poly(vinylidene fluoride) formation in poly(vinylidene fluoride)/poly(methyl methacrylate) blend from solutions, Appl. Surf. Sci. 254 (2008) 5635–5642.

[18] L. Yu, P. Cebe, Crystal polymorphism in electrospun composite nanofibers of poly(vinylidene fluoride) with nanoclay, Polymer 50 (2009) 2133–2141.
[19] V. Bharti, T. Kaura, R. Nath, Ferroelectric hysteresis in simultaneously stretched and corona-poled PVDF films, IEEE Trans. Dielect. Elect. Insulation 4 (1997) 738–741.
[20] K. Cramer, M. Fogliato santos lima, S.N. Magonov, E.H. Hellmann, M. Jacobs, G.P. Hellmann, J. Mater. Sci. 33 (1998) 2305–2312.
[21] J.C. Maxwell, A Treatise on Electricity and Magnetism, Dover Publ. Co., New York, 1954.
[22] T. Bhimasankaram, S.V. Suryanarayana, G. Prasad, Piezoelectric polymer composite materials, Curr. Sci. 74 (1998) 967–976.
[23] Y. Rao, J. Qu, T. Marinis, C.P. Wong, A precise numerical prediction of effective dielectric constant for polymer-ceramic composite based on effective-medium theory, IEEE Trans. Compon. Packag. Technol. 23 (2000) 680–683.
[24] S. Lanceros-Méndez, J.F. Mano, A.M. Costa, V.H. Schmidt, FTIR and DSC studies of mechanically deformed β-PVDF films, J. Macromol. Sci. Phys. B 40 (2001) 517–527.